

Do DALL-E and Flamingo Understand Each Other?

Hang Li^{*1,2} Jindong Gu^{*3} Rajat Koner¹ Sahand Sharifzadeh¹ Volker Tresp^{1,2}
¹LMU Munich, Germany ²Siemens AG, Germany ³University of Oxford, UK

Abstract

The field of multimodal research focusing on the comprehension and creation of both images and text has witnessed significant strides. This progress is exemplified by the emergence of sophisticated models dedicated to image captioning at scale, such as the notable Flamingo model and text-to-image generative models, with DALL-E serving as a prominent example. An interesting question worth exploring in this domain is whether Flamingo and DALL-E understand each other. To study this question, we propose a reconstruction task where Flamingo generates a description for a given image and DALL-E uses this description as input to synthesize a new image. We argue that these models understand each other if the generated image is similar to the given image. Specifically, we study the relationship between the quality of the image reconstruction and that of the text generation. We find that an optimal description of an image is one that gives rise to a generated image similar to the original one. The finding motivates us to propose a unified framework to finetune the text-to-image and image-to-text models. Concretely, the reconstruction part forms a regularization loss to guide the tuning of the models. Extensive experiments on multiple datasets with different image captioning and image generation models validate our findings and demonstrate the effectiveness of our proposed unified framework. As DALL-E and Flamingo are not publicly available, we use Stable Diffusion and BLIP in the remaining work. Project website: <https://dalleflamingo.github.io>.

1. Introduction

Recently, multimodal research that aims to improve machine understanding of images and text has made significant advances [42, 43, 46, 8, 38, 59, 67, 21]. Text-to-image generation models such as DALL-E [44, 43] and Stable Diffusion (SD) [46] are capable of converting complex textual descriptions [47] from real-world scenarios into high-fidelity images [43, 24, 40, 44]. Conversely, image-to-text generation models, e.g., Flamingo [2] and

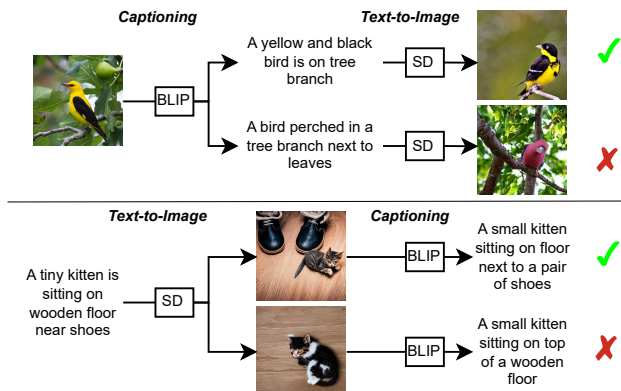


Figure 1. Illustration of the communication tasks between SD and BLIP. Top: SD generates an image for each caption created by BLIP, where an accurately reconstructed image indicates a more precise caption. Bottom: The reverse task involves SD generating image candidates, which are then used by BLIP to produce captions for those images. The best image that represents a text is the one that leads to the best reconstruction of the original text.

BLIP [35], exhibit the ability to comprehend the intricate semantics present in images and produce coherent descriptions [57, 26, 56, 55, 62, 37, 60]. Despite the closeness of the image captioning and text-to-image generation tasks, they are often studied in isolation from each other, i.e., the communication between these models is under-explored [38, 30]. This raises an interesting question: do image-to-text generation models and text-to-image generation models possess mutual understanding? Concretely, we investigate this question by letting an image-to-text model, BLIP, generate a text description for a given image, which subsequently serves as input to a text-to-image model, SD, to synthesize a new image¹. We argue that BLIP and SD understand each other if the generated image is similar to the source image. Such mutual understanding may enhance their respective abilities to comprehend underlying concepts, resulting in superior caption generation and image synthesis. Figure 1 illustrates this idea, where the upper caption is a better representation of the input image than the

^{*}Equal contribution. Correspondence to ha.li@campus.lmu.de

¹The initial idea of this work was motivated by Flamingo and DALL-E. However, their model weights are unavailable at the time of publication.

lower caption as it leads to a more faithful reconstruction of the original image.

To verify this assumption, we design two reconstruction tasks: image-text-image and text-image-text, shown in Figure 1. For the first reconstruction task, we evaluate the similarity between the semantics of the generated image and the input image, e.g., by computing the distance of image features extracted with a pretrained CLIP image encoder [42]. Afterward, we compare the generated text with human-annotated captions to assess the quality of the generated text [53]. Our experiments reveal that the quality of the reconstruction depends on the quality of the generated text. This leads to our first finding: the best description for an image is the description that enables the generative model to recreate the original image. Similarly, we design the reverse task where SD generates an image from a given text, and subsequently, BLIP produces a text from the generated image. We find that the best image representation for text is the one that generated the original text. We conjecture that through the reconstruction task, information on the input image is well preserved in the textual description and that meaningful description leads to a faithful recovery back to the image modality.

Based on our findings, we propose a novel finetuning framework that facilitates communication between text-to-image and image-to-text models, enabling them to talk to each other. Specifically, in our framework, a generative model not only receives training signals from human labels but also from a reconstruction loss. For a given image or text, one model first generates a representation of the input in the other modality and then the other model converts this representation back to the input modality. The reconstruction part forms a regularization loss to guide the finetuning of the first model. In this way, they acquire not only human supervision but also self-supervision that the generation should lead to a more accurate reconstruction. For example, the image captioning model should favor captions that not only match the labeled image-text pairs but also those that can lead to reliable reconstructions.

Our work is closely related to inter-agent communication. Language is a major means of exchanging information between agents. But how can we be sure that the first agent has the same understanding of what a cat or a dog is as the second agent? In this paper, we have the first agent analyze an image and produce a text describing that image. The second agent then obtains the text and simulates an image based on the text. This latter process can be thought of as an embodiment process [52]. We propose that communication is successful if the image simulated by the second agent is close to the image the first agent received as input. In essence, we test the effectiveness of language, which is the main communication venue of humans.

We conduct experiments leveraging the off-the-shelf

models [42, 35, 10, 45, 46, 64], in particular recently developed large-scale pre-trained image captioning models [35, 34] and image generation models [46, 64]. Extensive experiments demonstrated the advantages of our proposed framework for various generative models, in both training-free and finetuning settings. Specifically, in the training-free paradigm, our framework significantly enhanced the caption and image generation, whereas, for finetuning, we achieved improved results for both generative models. Our main contributions are summarized as follows:

- **Framework:** To the best of our knowledge, we are the first to explore the communication of standard alone image-to-text and text-to-image generative models through human-interpretable text and image representations. Contrastively, related work unifies image and text generation implicitly through an embedding space.
- **Findings:** We find that the quality of a caption can be evaluated by assessing the image reconstruction produced by a text-to-image model. The best caption for an image is one that leads to the most accurate reconstruction of the original image. Similarly, the best image for a caption is the image that leads to the best reconstruction of the original text.
- **Improvements:** Based on our findings, we propose a unified framework to enhance both the image-to-text and text-to-image models. This involves finetuning the image-to-text model using a reconstruction loss computed by a text-to-image model as regularization, and finetuning the text-to-image model using a reconstruction loss computed by an image-to-text model. We analyzed and verified the effectiveness of our framework.

2. Related Work

Text to Image Generation Popular text-conditioned image generation models mainly include GAN [19, 29, 28], VAE [31, 64, 14, 18, 61], and recently developed diffusion models [24, 40, 46, 43, 47, 5]. Diffusion models model image generation as a Markov Chain and learn the reversed process, where a noise vector is gradually denoised into an image [24]. For text-guided image generation, generative models compute the conditional probability of generating an image given the text. DALL-E [43] and SD [46] are representatives of such diffusion-based models that are scaled to real-world complexity. Such large-scale generative models are trained on an extensive amount of image-text pairs like the LAION [49] dataset obtained from the web. The utilization of large-scale datasets allows these models to generate a vast diversity of images from intricate text inputs. The focus of this work is specifically on examining the mutual understanding of these large-scale models.

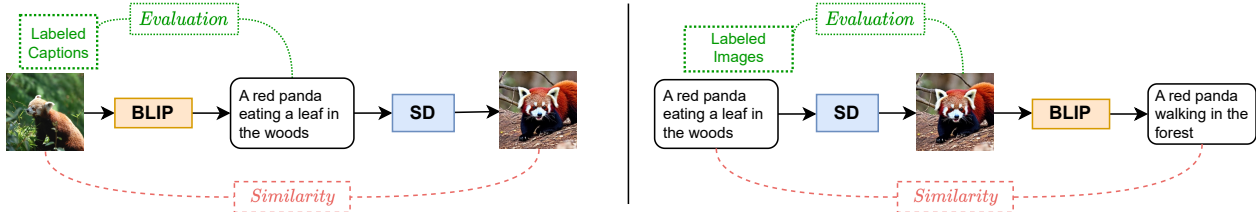


Figure 2. Illustration of our proposed inference framework. Left: a pipeline for image-text-image. The input image is fed to BLIP for caption generation and SD reconstructs the image from the generated text. The generated image is compared with the input image using a similarity function, e.g., based on image embeddings, which is utilized to evaluate the quality of the generated caption. We treat human-annotated captions as ground truth representations of the input image. Right: a pipeline for text-image-text. The reverse task for reconstructing text is demonstrated here.

Image Captioning Image captioning describes a scene using natural language [26, 56, 55, 62, 37, 60]. As one of the representatives of image captioning models, BLIP consists of an image encoder to understand the image features and a text decoder to generate text in an autoregressive manner. The image encoder uses a vision-transformer [15] backbone, which divides an image into a sequence of patches and outputs a sequence of embeddings that serve as the grounding information for text generation. Thereafter, a text decoder predicts the next token by attending to previous tokens and the encoded visual states. A recent trend in image captioning research is to develop large-scale visual language models that unify text generation with multiple image-text understanding tasks, e.g., image-based question answering and image-text retrieval [2, 13, 60]. We utilize BLIP as the image captioning method in this work.

Vision Language Representation Learning and Understanding Representation learning for vision and language handles semantic alignment between different modalities [51, 12, 13, 66, 7, 21]. A popular approach is to utilize contrastive learning on large-scale image and text pair datasets to obtain a unified representation of different representations for the same concept [42]. For unimodal image representation, self-supervised visual encoders, e.g., DINO [10], are proposed to encode visual semantics. For unimodal text representation, language models such as SBERT [45] can well extract semantics from the text. Several works have been proposed to enhance image and text generation by leveraging aligned image and text representations in the embedding space [38, 6, 58]. In contrast to their work, we aim to understand the representations learned by different image-to-text and text-to-image generative models using text or image as an interface.

3. Findings: Do BLIP and Stable Diffusion Understand Each Other?

In this section, we introduce two reconstruction tasks to test the mutual understanding of frozen BLIP and SD. We present our findings that a training-free reconstruction process can enhance the quality of a generated text or image.

3.1. Task Setup

Image-Text-Image This task aims to study the relationship between the quality of a reconstructed image and that of a caption. As shown on the left side of Figure 2, BLIP describes a given image in text, and SD generates an image from this description. Firstly, BLIP describes a source image x with different caption candidates $\{y^{(i)}\}_{i=1:N}$. When generating the captions, we use Top- p sampling [25] as the default sampling method while also examining two additional sampling strategies. Secondly, the captions are given to the SD to generate one image $\hat{x}^{(i)}$ for each caption $y^{(i)}$. We acquire N generated images for each input image. Finally, we compute the similarity between a generated image and its corresponding input image, as shown in red dashed lines in Figure 2. We utilize image embeddings obtained from pretrained encoders such as CLIP image encoder and DINO. The image encoder first encodes the input image x and a generated image $\hat{x}^{(i)}$ into embeddings space and the cosine similarity between the two embeddings is computed. We also experiment with additional image fidelity measures for a more solid evaluation.

Text-Image-Text Likewise, in the setting of *SD talking to BLIP*, shown on the right side of Figure 2, we investigate whether an improved text reconstruction corresponds to a superior image representation for a given text. We randomly sample a text from the image-text pair dataset and generate N images for each text using SD. Then BLIP generates a description for each input image using beam search [17]. Following this, we use different methods to calculate the similarity between the input and generated text, which is shown as the red dashed line in Figure 2. The similarity is computed with a text encoder where the alignment between two text embeddings extracted by the encoder is calculated. Two encoders are applied in our work. The first one is a multimodal text encoder, i.e., CLIP text encoder trained to align text and image features; The second one is a unimodal text encoder, i.e., SBERT [45] trained only on text data. Besides, traditional text similarity metrics like CIDEr [53] and WMD [33] between texts are also applied.

3.2. Evaluation Protocols

Evaluation Metric Image Captioning: We report standard metrics, including BLEU [41], CIDEr [53], SPICE [3], and WMD [33], as well as an embedding-based metric that computes the cosine distance between the embeddings of a candidate text and a human-labeled reference caption. For that, the CLIP text encoder and SBERT text encoder are used to obtain the caption embeddings. *Image Generation:* We use standard fidelity scores like FID [23] and Inception Score (IS) [48] to quantify the quality of the generated images. Similar to the caption evaluation, we also report embedding-based image distances between a generated and a real reference image. For that, we report the CLIP Visual Score similar to [32] and the DINO Score [10].

Implementation Details We set the number of caption candidates to $N=10$. The NoCaps [1] validation set and the COCO Karpathy test split [27] are used to support the evaluation. We randomly sample a caption for each image in the dataset for the input of the text-image-text task. All models are frozen in this section, without any finetuning. More implementation details can be found in Appendix A.

3.3. Findings

Insight I: a Better Caption is the One That Leads to a Better Visual Reconstruction. In the setting of image-text-image, we compute the captioning score of each generated text description, as well as the similarity score between the corresponding generated image and the input image. Then we rank the image similarities within N generated pairs for each input image and then aggregate the caption scores over the entire dataset. Figure 3 displays the correlation between the quality of the image reconstruction and the caption quality. Four scoring metrics and three similarity methods are analyzed in this experiment.

It is evident from Figure 3 that the reconstruction quality evaluated by a text-to-image model reveals the quality of the generated caption for the input image. Specifically, the better the reconstructed image, the better the caption score, independent of the similarity and the evaluation metrics. Moreover, DINO shows on-par performance with CLIP, even though DINO is trained only with image augmentations and contrastive learning on the pixel space. This rules out the possibility that CLIP might influence the comparison since it is trained to align multimodal image-text features. Furthermore, we obtain consistent results for both embedding-based captioning metrics and word frequency matching metrics.

Quantitatively, we compare our method with the baseline sampling method. For baseline, we repeat the sampling multiple times and average the final captioning metric. As shown in Table 1, our approach consistently produces better captions. The relative gain is more significant for No-

Caps, especially for the out-domain subset, which contains novel objects that usually require accurate concepts to describe. The choice of the hyperparameter for the baseline sampling method is discussed in Appendix B. Additionally, we find our conclusion consistent for two different sampling strategies widely used for captioning (See Appendix C). The number of candidates N has minimal impact on the conclusion and is discussed in Appendix D.

Qualitatively, we observed plausible improvements. Our approach accurately describes the bird in Figure 5 with detailed attributes. More figures are in Appendix E.

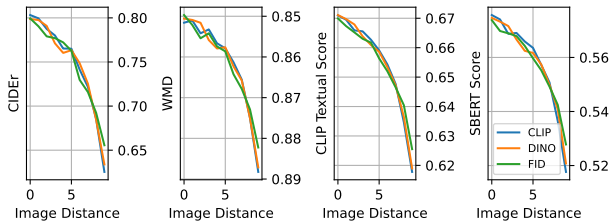


Figure 3. Evaluation of the image-text-image pipeline with three similarity and four caption metrics on the NoCaps dataset. The result suggests that regardless of the similarity or evaluation metric, better image reconstruction always leads to better captions.

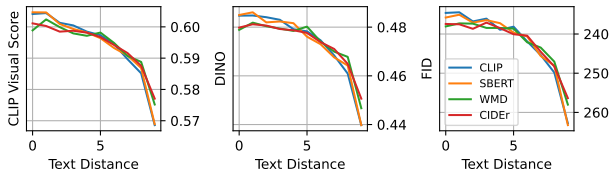


Figure 4. Evaluation of the text-image-text pipeline with four types of similarity and three types of evaluation metrics on the NoCaps dataset. The result is consistent for all types of combinations.

Insight II: a Better Image is the One That Leads to a Better Text Reconstruction. Similarly, we find that text reconstruction boosts the quality of text-to-image generation. As shown in Figure 4, when the reconstructed text is dissimilar to the original text, on average the image quality is low. In contrast, high-quality reconstruction is associated with a high-quality image. This holds true for both the fidelity and semantic metrics on image generation evaluation. For different similarity functions, we find that embedding-based similarity methods, i.e., CLIP and SBERT, perform better than similarity metrics based on word co-occurrence, i.e., CIDEr and WMD. Table 2 demonstrates the quantitative improvement of our method compared to the baseline in terms of fidelity and semantic alignment. Additionally, we present a qualitative example in Figure 5. The last image does not properly represent the input text describing a piece of cheesecake, which leads to an inaccurate caption in the next step. By comparing the generated captions with the in-

Method	Nocaps								COCO			
	In-domain		Near-domain		Out-domain		Overall		Karpathy Test			
	CIDEr	SPICE	CIDEr	SPICE	CIDEr	SPICE	CIDEr	SPICE	B@3	B@4	CIDEr	SPICE
Baseline Sampling	75.1	12.4	72.4	11.9	78.7	11.5	74.1	11.9	32.4	21.9	90.1	19.6
Ours	77.3	12.9	78.3	12.6	88.8	12.4	80.3	12.6	32.5	22.0	92.0	20.1
Gain (%)	+2.9	+4.0	+8.1	+5.9	+12.8	+7.8	+8.4	+5.9	+0.4	+0.3	+2.1	+2.2

Table 1. Comparison of the baseline captioning model and our proposed method on Nocaps and COCO datasets. Our method outperforms the baseline sampling method on all metrics. The relative gain of our method compared to the sampling method is given in the third row. B@k: BLEU@k.

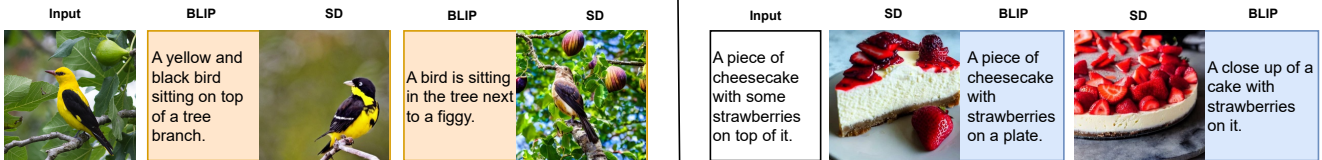


Figure 5. Qualitative examples of reconstruction tasks. The left side shows image reconstruction for the given input image of a bird. Two samples are shown with their generated images, ranked by the image similarity. The right side shows text reconstruction whereas the first sample gives a high-quality image as well as high-quality text reconstruction.

Model	NoCaps			COCO		
	CLIP↓	FID↓	IS↑	CLIP↓	FID↓	IS↑
Sampling	40.54	32.37	41.19	42.54	44.76	30.01
Ours	33.47	29.59	45.64	34.74	42.02	31.62
Gain (%)	+17.4	+8.6	+9.8	+18.3	+6.1	+5.4

Table 2. Comparison of our proposed method to SD on image generation. Our method uses BLIP to filter out generated images based on text reconstruction.

put text, we find better images that faithfully depict the text. These examples highlight the finding that an image-to-text model can be used to assess the quality of a generated image, i.e., the more similar the reconstructed text to the input text, the higher the quality of the generated image.

Additional experiments with different image captioning and text-to-image generation models in Appendix F lead to the same conclusion for the two tasks.

4. Method: Let BLIP and Stable Diffusion Talk

Based on the insights in the last section, we introduce a novel approach to finetuning the image captioning and text-to-image models by incorporating reconstructions as regularization losses. Similar to the last section, we introduce two pipelines: image-text-image and text-image-text. In the first pipeline, BLIP generates a caption for a given image, where SD is guided by this caption to reconstruct the input image. The core component is a differentiable layer that connects the output of the BLIP with the input of SD. This connection allows optimizing BLIP using the loss computed by SD in the text-to-image generation process. Likewise, in the second pipeline, we optimize the SD model using the loss obtained from comparing the generated text by BLIP with the input text. A schematic of our training framework is presented in Figure 6 and explained below.

4.1. Image-Text-Image

Text Generation Stage The left box in Figure 6 (a) illustrates the standard image captioning process using the BLIP model. BLIP takes an image $x \in \mathbb{R}^{H \times W \times 3}$ in RGB space as input and produces a sequence of tokens y_t . The prediction of each token y_t at time step t relies on tokens generated in previous steps $y_{<t}$ and the image embeddings. To accelerate the training using batch operation, a ground-truth caption y is fed to BLIP with an attention mask, ensuring that each token’s prediction is causally dependent on the tokens that came before it. In this way, BLIP can generate a caption for an input image using only a single forward pass during training. Therefore, the training objective of the image captioning model is to minimize the cross-entropy loss between the ground truth text and the predicted text, defined as

$$\mathcal{L}_{TG} = \mathbb{E}_{x, y \sim \mathcal{D}} [\Pi_t p_\theta(y_t | y_{<t}, x)], \quad (1)$$

where θ refers to the weights of BLIP and \mathcal{D} refers to the dataset from which a ground-truth image-text pair (x, y) is sampled. The BLIP model was pretrained using \mathcal{L}_{TG} . Throughout the finetuning process, this loss is further utilized to update the weights of BLIP, preventing its predictions from deviating from the text used in pretraining.

Differentiable Connection The final softmax layer of BLIP generates a token distribution $\hat{g}_t \in \mathbb{R}^V$ at each timestep which is used to decode a discrete token y_t during image captioning. V represents the size of the vocabulary of a tokenizer. However, instead of sampling a specific y_t at each step, we store the token distributions $\hat{g} \in \mathbb{R}^{L \times V}$ for all timesteps, where L is the number of tokens in a caption. During the training phase, this can be obtained after a forward process of the input image. Subsequently, we compute the dot product of the token distributions \hat{g} with the vo-

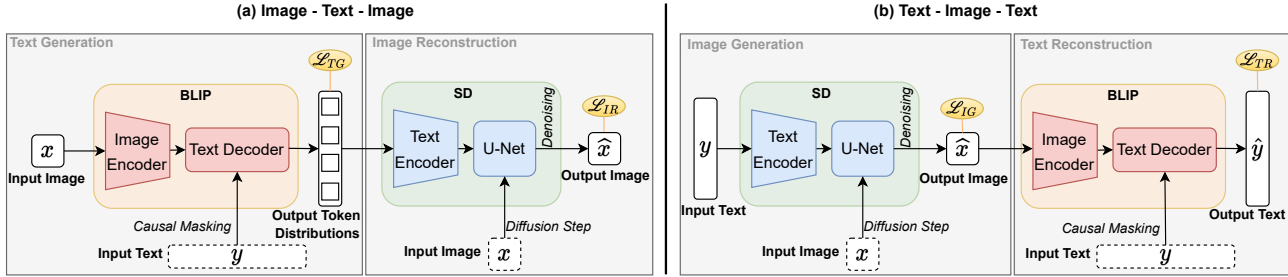


Figure 6. Illustration of our proposed finetuning framework. We introduce a reconstruction pipeline starting from an image (left) and a reconstruction pipeline starting from the text (right). Input images and text shown at the bottom (dashed boxes) are only used during training and will be dropped during inference. For illustration proposes, we omit the VAE in SD without changing the principles. Causal masking is a technique for language modeling during training. The diffusion step denotes adding noise to the input image.

cabulary embeddings $E \in \mathbb{R}^{V \times D}$ of SD’s tokenizer. This produces text embeddings, which are used to guide image generation. Later stages follow the standard text-to-image generation pipeline.

In addition, to address the discrepancy between the tokenizers used by BLIP and SD, we employ a hard-coded transformation matrix to map the vocabulary of BLIP’s tokenizer to that of SD (See Appendix G). For future work, we will explore discrete sampling methods for caption generation. In this work, we stick to our simple strategy as it has proven to be useful in practice.

Image Reconstruction Stage The right box of Figure 6 (a) shows the conventional procedure of training a text-guided image generative diffusion model. The model is trained on an input image x along with its textual description y . The training procedure involves a forward diffusion process wherein a clean image is progressively destructed by introducing noise in iterative steps. Then SD learns a reversed process where it predicts the noise that is necessary to reconstruct the denoised image for each step. In the context of text-to-image generation, the input text y is processed by the text encoder as conditional information to guide this reversed denoising process.

Specifically, for the diffusion process, a noise vector ϵ for timestep t is sampled from a normal distribution. A noised image x_t of the original clean image x_0 for timestep t is computed following a predefined noise scheduling process denoted as $x_t = \sqrt{\alpha_t}x_0 + \sqrt{1 - \alpha_t}\epsilon$, where α_t is a predefined scalar value for noise scheduling. The U-Net² of SD predicts ϵ from x_t , t , and the encoding of the text input c . Formally, the training objective of SD is to minimize a mean squared error (MSE), defined as $\mathcal{L} = \mathbb{E}_{x,y \sim \mathcal{D}, t \sim [1,T]} [\|\hat{\epsilon}_\psi(x_t, t, c) - \epsilon\|^2]$, where ψ represents the weights of SD and T is a fixed number for diffusion steps. SD uses a CLIP text encoder π to encode the

²In fact, SD utilizes a variational autoencoder to compress the image into a latent space and subsequently learns the diffusion process in that space. For more details, readers are referred to [46].

text y , written as $c = \pi(y)$. In our proposed approach, the encoding is obtained using $c = \pi(\hat{y})$, which incorporates the modification introduced in the preceding subsection. In summary, the image reconstruction loss is,

$$\mathcal{L}_{IR} = \mathbb{E}_{x,y \sim \mathcal{D}, t \sim [1,T]} [\|\hat{\epsilon}_\psi(x, t, \pi(\hat{y})) - \epsilon\|^2]. \quad (2)$$

Intuitively, if a caption is of high quality in describing the content of the input image, SD is expected to have a lower loss in reconstructing that image. During training, we uniformly sample a timestep t for each predicted caption.

In contrast to the approach outlined in Section 3.1, our novel design does not require an extra image encoder since the input image is already incorporated into the generation process of SD. This aligns with the standard training procedure, where SD reconstructs a given ground-truth image rather than generating a new image from scratch. Directly converting the approach in Section 3.1 into a training framework would be impractical as it requires a costly sampling procedure.

4.2. Text-Image-Text

Image Generation Stage This stage is equivalent to the conventional training of SD described above. Similar to Eq. 2, the loss is defined as

$$\mathcal{L}_{IG} = \mathbb{E}_{x,y \sim \mathcal{D}, t \sim [1,T]} [\|\hat{\epsilon}_\psi(x_t, t, \pi(y)) - \epsilon\|^2]. \quad (3)$$

However, this procedure does not directly produce a clean image, which is required as input for BLIP. For that, we adopt the 1-step approximation [36, 54] technique for diffusion models. Specifically, based on the noisy image x_t and SD’s predicted noise $\hat{\epsilon} = \hat{\epsilon}_\psi(x_t, t, \pi(y))$, a clean image \hat{x}_0 can be recovered by $\hat{x}_0 = \frac{1}{\sqrt{\alpha_t}}(x_t - \sqrt{1 - \alpha_t}\hat{\epsilon})$. During training, for each sampled timestep t , we predict \hat{x}_0 and feed the prediction to BLIP for caption generation.

Text Reconstruction Stage The BLIP takes the predicted image \hat{x}_0 as input and produces a caption. Following the

Method	Nocaps									COCO			
	I-C	N-C	O-C	B@1	B@2	B@3	B@4	CIDEr	SPICE	B@3	B@4	CIDEr	SPICE
BLIP ViT-B [35]	111.8	108.6	111.5	83.6	68.2	50.6	32.0	109.7	14.7	50.5	39.7	133.3	23.8
Ours ViT-B, SD	114.9	110.8	112.9	84.6	69.4	51.9	32.9	111.8	14.9	51.4	40.1	134.6	24.0
BLIP ViT-L [35]	114.9	112.1	115.3	84.2	69.3	51.7	33.1	113.2	14.8	51.4	40.4	136.7	24.3
Ours ViT-L, SD	116.1	113.0	115.6	84.7	70.0	52.5	33.6	114.0	14.9	52.0	40.9	137.3	24.1
BLIP-2 [34]	122.7	118.0	123.8	86.8	73.2	56.2	37.0	119.9	15.4	55.5	43.7	145.8	25.2
Ours BLIP-2, SD	123.8	119.3	124.2	86.9	73.5	56.5	37.1	121.0	15.4	56.0	44.1	146.4	25.2

Table 3. Evaluation results of image captioning. We conduct experiments with different image captioning models (BLIP ViT-B, BLIP ViT-L, BLIP-2) with an image generation model (SD). I-C/N-C/O-C: In-/Near-/Out-domain CIDEr. The remaining metrics are on the entire set. B@k: BLEU@k.

same procedure in the text generation stage, the text reconstruction loss is defined as

$$\mathcal{L}_{TR} = \mathbb{E}_{x,y \sim \mathcal{D}} [\Pi_t p_\theta(y_t | y_{<t}, \hat{x}_0)]. \quad (4)$$

The major difference is that \mathcal{L}_{TR} is conditioned on images with gradients originating from SD, which allows optimizing SD’s parameters by BLIP’s loss.

4.3. Full Training Objective

We simplify the training pipelines by adding the individual losses into a single training loss, and then optimizing both models on this summed loss. The parameters of both models are updated at each iteration, enabling a joint improvement of both models.

$$\mathcal{L}(\theta, \psi) = \mathcal{L}_{TG} + \mathcal{L}_{IR} + \mathcal{L}_{IG} + \mathcal{L}_{TR}. \quad (5)$$

See Appendix H for a discussion on our loss function, including its connection to CycleGAN [65], and the pseudo-code for the training framework.

5. Experimental Setup

Dataset and Evaluation *Training dataset:* We finetune both BLIP and SD on the COCO Karpathy train split [27] of 113k images, each associated with five captions. *Image Captioning:* Following [35], the image captioning is evaluated on the COCO test set and NoCaps validation set, utilizing metrics described in Section 3.2. Unlike the COCO dataset, which contains images with common object categories, the NoCaps dataset includes images in the wild, making it a challenging benchmark for zero-shot evaluation for image captioning. *Image Generation:* For image generation, we report the CLIP image distance, defined in Section 3.2, on the COCO test set and the NoCaps validation set. Likewise, the NoCaps dataset is used as a zero-shot evaluation benchmark. As each image is associated with multiple captions, we randomly sample a caption for each image to construct these two test sets.

Baselines and Models *Image Captioning:* BLIP ViT-B denotes the BLIP model with ViT-B/16 as the visual backbone. BLIP ViT-L uses a larger variant of ViT, i.e., ViT-L/16. We use the bootstrapped and finetuned version since they are optimized to produce the best baselines for captioning. We further explore the BLIP-2 ViT-G OPT_{2.7B} which is among the SOTA captioning methods. We do not further finetune their models as they have already been finetuned on the same dataset using text generation loss. Thus we use performance metrics reported from their paper [35, 34]. For the metrics that are not available, we run the evaluation with their published code and weights to get the results. *Image Generation:* Since, as of this writing, we have not found any other publicly available text-to-image generation models with on-par performance, we utilize SD as the baseline model. We use the weights of sd-v1-4.ckpt for SD. The output image size is 512 except for BLIP-2, where we down-scaled the image size to 384 due to hardware constraints. Since SD is not trained on the COCO dataset, we finetune SD using MSE loss to serve as a baseline method.

For our finetuning framework, we conducted experiments with the combinations of the three above-mentioned image captioning models and the text-to-image model. For the ablation study, we use BLIP ViT-B as the default setting.

Training Details To improve the efficiency, we finetune a subset of weights of SD and BLIP following heuristics [32] and hyperparameter search. For BLIP ViT-B and ViT-L, we finetune the query projection weights in the cross-attention layer of the text decoder and freeze the other components. For BLIP-2, the query tokens are adapted. For SD, we finetune the query projection weights in the cross-attention layer. Unless specified, we use a learning rate of 1e-4 and batch size of 8 and finetune the framework for 5 epochs. The experiments are conducted on an A10 GPU with 24GB of memory. The finetuning is efficient, requiring only a forward pass for both BLIP and SD per input. Thus, the additional computations introduced by the reconstruction process are relatively minor, amounting to approximately 1.4 times the original cost.

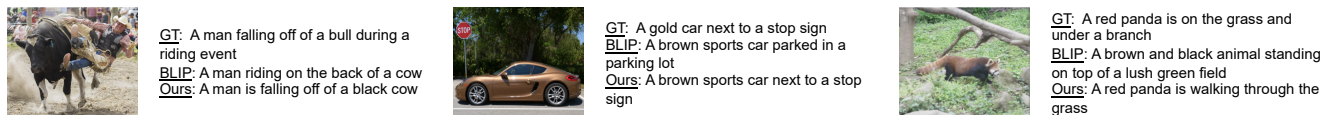


Figure 7. Qualitative evaluation of image captioning. From top to down, we show a ground-truth (GT) caption, a generated caption from BLIP ViT-B, and a generated caption from our finetuned model of ViT-B.



Figure 8. Qualitative evaluation of image generation. The left side shows a textual input and a reference image. The upper images on the right side are generated by the SD baseline. The lower images are generated from our model.

6. Evaluation Results

Here we present a comprehensive evaluation of our framework by comparing it to baselines and showing qualitative results. In addition, we discuss and analyze our training objective.

Improvement in Image Captioning Table 3 shows the performance of different models on the image captioning task. We report a broader set of metrics on the entire dataset for a more detailed evaluation. As shown in the table, our finetuned model demonstrated improved performance across most metrics. Our approach is effective across different sizes (ViT-B vs ViT-L) and architectures (BLIP vs BLIP-2) of image captioning models. Note that our model outperforms ViT-B with a 2% improvement in CIDEr, which is a larger gain compared to BLIP’s 0.7% improvement obtained through bootstrapping on a dataset of 129M images.

Improvement in Image Generation Similarly, we compare the performance of text-to-image generation models in Table 4. We observe that SD finetuned with our reconstruction loss can produce more semantically aligned images on the NoCaps dataset that contains diverse and real-world scenarios, despite slightly reduced fidelity. Finetuning SD solely with MSE loss on human-labeled image-text pairs yields improvements in the COCO test set, which has the same data distribution as the training data. However, this approach leads to worse performance in image fidelity and degraded alignment on the NoCaps dataset. In general, utilizing reconstruction loss leads to improvements over human supervision. Our proposed framework has demonstrated significant potential to improve image generation.

Qualitative Results Our method generates a more faithful description of a scene in terms of relationships, context, and fine-grained concepts. For example, BLIP correctly recog-

Model	NoCaps		COCO	
	CLIP ↓	FID ↓	CLIP ↓	FID ↓
SD [46]	0.4039	21.19	0.4248	27.08
SD MSE	0.4077	24.32	0.4011	25.66
Ours ViT-B, SD	0.3978	21.96	0.4068	24.68
Ours ViT-L, SD	0.4031	22.92	0.4071	24.21

Table 4. Evaluation results of image generation. We compare baseline methods, SD and MSE loss, with our image generation models that are finetuned with two image captioning models.

nizes the objects in the left-most image in Figure 7, but it fails to predict the relationship between them. In contrast, our model generates a correct description, likely driven by the reconstruction loss that the visual perception of a man riding a cow is different from that of a man falling off a cow. In addition, Figure 8 shows an example of generated images using our model and SD baseline method. The baseline may neglect certain objects like the car, whereas our method reflects the text prompt. More figures are in Appendix J.

Captioning			Image Generation		
Model	CIDEr	SPICE	Model	CLIP ↓	FID ↓
Ours	111.8	14.9	Ours	0.3978	21.96
w/o \mathcal{L}_{TG}	102.3	14.0	w/o \mathcal{L}_{IG}	0.4241	26.56
w/o \mathcal{L}_{IR}	109.7	14.7	w/o \mathcal{L}_{TR}	0.4077	24.32

Table 5. Analysis of the loss function. We conduct experiments with either only the regularization loss or only the supervision of image-text pairs.

Analysis of Loss Function We investigate the effectiveness of our proposed loss function, especially examining if the reconstruction loss alone can still lead to the improvement exhibited above. The first row in Table 5 shows the results of our final models trained on the combined pipelines using Eq. 5, whereas for the second and third rows, we separately train the two pipelines and ablate the loss terms. The second row on the left side of the table refers to the BLIP model trained solely on \mathcal{L}_{IR} using the framework in Figure 6 (a). As expected, the model struggles to provide competitive results. This shows the benefit of human supervision, which prevents the model from overfitting the reconstruction objective. For completeness, we also show the performance of BLIP with only the image captioning objective in the third row of Table 5. As our training framework involves different loss terms and finetuning strategies, a more detailed analysis of those aspects can be found in Appendix I.

7. Discussions and Limitations

Besides our findings and improvements, this work also opens up avenues for potential future directions. 1) The novel design of backpropagating through SD allows image generation to be used as a downstream task, wherein the knowledge in diffusion models is effectively transferred. 2) The findings in our work inspire the development of label-free evaluation metrics for image captioning.

The primary limitation of this work is the restricted scope of improvement. In our work, the degree of improvement in BLIP and SD depends on their initial capacities. As a result, challenges may remain for complex images or intricate descriptions which are not well covered in the data distribution for pretraining. Besides, we treat the transformations from image to text and text to image as a black box, lacking a deeper understanding of the alignment between layers within models in the generation processes. We leave further exploration with explanation methods in future work [50, 4, 22]. Another under-explored perspective is the robustness of our finetuning paradigm. Concretely, it is not clear how the fine-tuned models perform under out-of-distribution images and texts [20, 11]. Additionally, our work also inherits the known limitations of large-scale generative models [2, 63], bringing concerns about possible biases or harmful content generation.

8. Conclusion

In this work, we investigated mutual understanding between multimodal image-to-text models and text-to-image models through image-text-image and text-image-text reconstruction tasks. We found that the reconstruction quality of text-to-image and image-to-text models can be utilized to evaluate the quality of the text or image generation. Specifically, the best textual description for an image is one that leads to a better reconstruction of the input image. The best image representation of text input is one that leads to a better recovery of the original text. Leveraging these findings, we proposed a novel framework for finetuning the image captioning and image generation models. We demonstrated enhanced performance of our models on both tasks. Our work advocates further exploring multimodal communication between text-to-image and image-to-text models. Finally, our work demonstrated the value of symbolic sentences to convey information: Image content can effectively be compressed into a sentence, and a sentence can be reconstructed as an image. This latter step can be considered a form of grounded cognition or embodiment.

References

[1] Harsh Agrawal, Karan Desai, Yufei Wang, Xinlei Chen, Rishabh Jain, Mark Johnson, Dhruv Batra, Devi Parikh, Stefan Lee, and Peter Anderson. Nocaps: Novel object caption-

ing at scale. In *Proceedings of the IEEE/CVF International Conference on Computer Vision*, pages 8948–8957, 2019. 4, 13

[2] Jean-Baptiste Alayrac, Jeff Donahue, Pauline Luc, Antoine Miech, Iain Barr, Yana Hasson, Karel Lenc, Arthur Mensch, Katie Millican, Malcolm Reynolds, et al. Flamingo: a visual language model for few-shot learning. *arXiv preprint arXiv:2204.14198*, 2022. 1, 3, 9

[3] Peter Anderson, Basura Fernando, Mark Johnson, and Stephen Gould. Spice: Semantic propositional image caption evaluation. In *European conference on computer vision*, pages 382–398. Springer, 2016. 4

[4] Sebastian Bach, Alexander Binder, Grégoire Montavon, Frederick Klauschen, Klaus-Robert Müller, and Wojciech Samek. On pixel-wise explanations for non-linear classifier decisions by layer-wise relevance propagation. *PLoS one*, 10(7):e0130140, 2015. 9

[5] Yogesh Balaji, Seungjun Nah, Xun Huang, Arash Vahdat, Jiaming Song, Karsten Kreis, Miika Aittala, Timo Aila, Samuli Laine, Bryan Catanzaro, et al. ediffi: Text-to-image diffusion models with an ensemble of expert denoisers. *arXiv preprint arXiv:2211.01324*, 2022. 2

[6] Fan Bao, Shen Nie, Kaiwen Xue, Chongxuan Li, Shi Pu, Yaole Wang, Gang Yue, Yue Cao, Hang Su, and Jun Zhu. One transformer fits all distributions in multi-modal diffusion at scale. *arXiv preprint arXiv:2303.06555*, 2023. 3

[7] Hangbo Bao, Wenhui Wang, Li Dong, Qiang Liu, Owais Khan Mohammed, Kriti Aggarwal, Subhojit Som, and Furu Wei. Vlmo: Unified vision-language pre-training with mixture-of-modality-experts. *arXiv preprint arXiv:2111.02358*, 2021. 3

[8] Khaled Bayouh, Raja Knani, Fayçal Hamdaoui, and Abdelatif Mtibaa. A survey on deep multimodal learning for computer vision: advances, trends, applications, and datasets. *The Visual Computer*, pages 1–32, 2021. 1

[9] Massimo Caccia, Lucas Caccia, William Fedus, Hugo Larochelle, Joelle Pineau, and Laurent Charlin. Language gans falling short. *arXiv preprint arXiv:1811.02549*, 2018. 13

[10] Mathilde Caron, Hugo Touvron, Ishan Misra, Hervé Jégou, Julien Mairal, Piotr Bojanowski, and Armand Joulin. Emerging properties in self-supervised vision transformers. In *Proceedings of the IEEE/CVF international conference on computer vision*, pages 9650–9660, 2021. 2, 3, 4

[11] Shuo Chen, Jindong Gu, Zhen Han, Yunpu Ma, Philip Torr, and Volker Tresp. Benchmarking robustness of adaptation methods on pre-trained vision-language models. *arXiv preprint arXiv:2306.02080*, 2023. 9

[12] Yen-Chun Chen, Linjie Li, Licheng Yu, Ahmed El Kholy, Faisal Ahmed, Zhe Gan, Yu Cheng, and Jingjing Liu. Uniter: Learning universal image-text representations. 2019. 3

[13] Jaemin Cho, Jie Lei, Hao Tan, and Mohit Bansal. Unifying vision-and-language tasks via text generation. In *International Conference on Machine Learning*, pages 1931–1942. PMLR, 2021. 3

[14] Ming Ding, Zhuoyi Yang, Wenyi Hong, Wendi Zheng, Chang Zhou, Da Yin, Junyang Lin, Xu Zou, Zhou Shao,

- Hongxia Yang, et al. Cogview: Mastering text-to-image generation via transformers. *Advances in Neural Information Processing Systems*, 34:19822–19835, 2021. 2
- [15] Alexey Dosovitskiy, Lucas Beyer, Alexander Kolesnikov, Dirk Weissenborn, Xiaohua Zhai, Thomas Unterthiner, Mostafa Dehghani, Matthias Minderer, Georg Heigold, Sylvain Gelly, et al. An image is worth 16x16 words: Transformers for image recognition at scale. *arXiv preprint arXiv:2010.11929*, 2020. 3
- [16] Angela Fan, Mike Lewis, and Yann Dauphin. Hierarchical neural story generation. *arXiv preprint arXiv:1805.04833*, 2018. 13
- [17] Markus Freitag and Yaser Al-Onaizan. Beam search strategies for neural machine translation. *ACL 2017*, page 56, 2017. 3
- [18] Oran Gafni, Adam Polyak, Oron Ashual, Shelly Sheynin, Devi Parikh, and Yaniv Taigman. Make-a-scene: Scene-based text-to-image generation with human priors. In *Computer Vision—ECCV 2022: 17th European Conference, Tel Aviv, Israel, October 23–27, 2022, Proceedings, Part XV*, pages 89–106. Springer, 2022. 2
- [19] Ian Goodfellow, Jean Pouget-Abadie, Mehdi Mirza, Bing Xu, David Warde-Farley, Sherjil Ozair, Aaron Courville, and Yoshua Bengio. Generative adversarial networks. *Communications of the ACM*, 63(11):139–144, 2020. 2
- [20] Jindong Gu, Ahmad Beirami, Xuezhi Wang, Alex Beutel, Philip Torr, and Yao Qin. Towards robust prompts on vision-language models. *arXiv preprint arXiv:2304.08479*, 2023. 9
- [21] Jindong Gu, Zhen Han, Shuo Chen, Ahmad Beirami, Bailan He, Gengyuan Zhang, Ruotong Liao, Yao Qin, Volker Tresp, and Philip Torr. A systematic survey of prompt engineering on vision-language foundation models. *arXiv preprint arXiv:2307.12980*, 2023. 1, 3
- [22] Jindong Gu, Yinchong Yang, and Volker Tresp. Understanding individual decisions of cnns via contrastive backpropagation. In *Computer Vision—ACCV 2018: 14th Asian Conference on Computer Vision, Perth, Australia, December 2–6, 2018, Revised Selected Papers, Part III 14*, pages 119–134. Springer, 2019. 9
- [23] Martin Heusel, Hubert Ramsauer, Thomas Unterthiner, Bernhard Nessler, and Sepp Hochreiter. Gans trained by a two time-scale update rule converge to a local nash equilibrium. *Advances in neural information processing systems*, 30, 2017. 4
- [24] Jonathan Ho, Ajay Jain, and Pieter Abbeel. Denoising diffusion probabilistic models. *Advances in Neural Information Processing Systems*, 33:6840–6851, 2020. 1, 2
- [25] Ari Holtzman, Jan Buys, Li Du, Maxwell Forbes, and Yejin Choi. The curious case of neural text degeneration. *arXiv preprint arXiv:1904.09751*, 2019. 3
- [26] MD Zakir Hossain, Ferdous Sohel, Mohd Fairuz Shiratuddin, and Hamid Laga. A comprehensive survey of deep learning for image captioning. *ACM Computing Surveys (CSUR)*, 51(6):1–36, 2019. 1, 3
- [27] Andrej Karpathy and Li Fei-Fei. Deep visual-semantic alignments for generating image descriptions. In *Proceedings of the IEEE conference on computer vision and pattern recognition*, pages 3128–3137, 2015. 4, 7, 13
- [28] Tero Karras, Samuli Laine, and Timo Aila. A style-based generator architecture for generative adversarial networks. In *Proceedings of the IEEE/CVF conference on computer vision and pattern recognition*, pages 4401–4410, 2019. 2
- [29] Tero Karras, Samuli Laine, Miika Aittala, Janne Hellsten, Jaakko Lehtinen, and Timo Aila. Analyzing and improving the image quality of stylegan. In *Proceedings of the IEEE/CVF conference on computer vision and pattern recognition*, pages 8110–8119, 2020. 2
- [30] Taehoon Kim, Gwangmo Song, Sihaeng Lee, Sangyun Kim, Yewon Seo, Soonyoung Lee, Seung Hwan Kim, Honglak Lee, and Kyunghoon Bae. L-verse: Bidirectional generation between image and text. In *Proceedings of the IEEE/CVF Conference on Computer Vision and Pattern Recognition*, pages 16526–16536, 2022. 1
- [31] Diederik P Kingma and Max Welling. Auto-encoding variational bayes. *stat*, 1050:1, 2014. 2
- [32] Nupur Kumari, Bingliang Zhang, Richard Zhang, Eli Shechtman, and Jun-Yan Zhu. Multi-concept customization of text-to-image diffusion. *arXiv preprint arXiv:2212.04488*, 2022. 4, 7
- [33] Matt Kusner, Yu Sun, Nicholas Kolkin, and Kilian Weinberger. From word embeddings to document distances. In Francis Bach and David Blei, editors, *Proceedings of the 32nd International Conference on Machine Learning*, volume 37 of *Proceedings of Machine Learning Research*, pages 957–966, Lille, France, 07–09 Jul 2015. PMLR. 3, 4
- [34] Junnan Li, Dongxu Li, Silvio Savarese, and Steven Hoi. Blip-2: Bootstrapping language-image pre-training with frozen image encoders and large language models. *arXiv preprint arXiv:2301.12597*, 2023. 2, 7, 14
- [35] Junnan Li, Dongxu Li, Caiming Xiong, and Steven Hoi. Blip: Bootstrapping language-image pre-training for unified vision-language understanding and generation. *arXiv preprint arXiv:2201.12086*, 2022. 1, 2, 7, 13, 14
- [36] Wei Li, Xue Xu, Xinyan Xiao, Jiachen Liu, Hu Yang, Guohao Li, Zhanpeng Wang, Zhifan Feng, Qiaoqiao She, Yajuan Lyu, et al. Upainting: Unified text-to-image diffusion generation with cross-modal guidance. *arXiv preprint arXiv:2210.16031*, 2022. 6
- [37] Xiujun Li, Xi Yin, Chunyuan Li, Pengchuan Zhang, Xiaowei Hu, Lei Zhang, Lijuan Wang, Houdong Hu, Li Dong, Furu Wei, et al. Oscar: Object-semantics aligned pre-training for vision-language tasks. In *Computer Vision—ECCV 2020: 16th European Conference, Glasgow, UK, August 23–28, 2020, Proceedings, Part XXX 16*, pages 121–137. Springer, 2020. 1, 3
- [38] Jiasen Lu, Christopher Clark, Rowan Zellers, Roozbeh Motlaghi, and Aniruddha Kembhavi. Unified-io: A unified model for vision, language, and multi-modal tasks. *arXiv preprint arXiv:2206.08916*, 2022. 1, 3
- [39] Moin Nadeem, Tianxing He, Kyunghyun Cho, and James Glass. A systematic characterization of sampling algorithms for open-ended language generation. *arXiv preprint arXiv:2009.07243*, 2020. 13

- [40] Alex Nichol, Prafulla Dhariwal, Aditya Ramesh, Pranav Shyam, Pamela Mishkin, Bob McGrew, Ilya Sutskever, and Mark Chen. Glide: Towards photorealistic image generation and editing with text-guided diffusion models. *arXiv preprint arXiv:2112.10741*, 2021. 1, 2
- [41] Kishore Papineni, Salim Roukos, Todd Ward, and Wei-Jing Zhu. Bleu: a method for automatic evaluation of machine translation. In *Proceedings of the 40th annual meeting of the Association for Computational Linguistics*, pages 311–318, 2002. 4
- [42] Alec Radford, Jong Wook Kim, Chris Hallacy, Aditya Ramesh, Gabriel Goh, Sandhini Agarwal, Girish Sastry, Amanda Askell, Pamela Mishkin, Jack Clark, et al. Learning transferable visual models from natural language supervision. In *International Conference on Machine Learning*, pages 8748–8763. PMLR, 2021. 1, 2, 3
- [43] Aditya Ramesh, Prafulla Dhariwal, Alex Nichol, Casey Chu, and Mark Chen. Hierarchical text-conditional image generation with clip latents. *arXiv preprint arXiv:2204.06125*, 2022. 1, 2
- [44] Aditya Ramesh, Mikhail Pavlov, Gabriel Goh, Scott Gray, Chelsea Voss, Alec Radford, Mark Chen, and Ilya Sutskever. Zero-shot text-to-image generation. In *International Conference on Machine Learning*, pages 8821–8831. PMLR, 2021. 1
- [45] Nils Reimers and Iryna Gurevych. Sentence-bert: Sentence embeddings using siamese bert-networks. *arXiv preprint arXiv:1908.10084*, 2019. 2, 3
- [46] Robin Rombach, Andreas Blattmann, Dominik Lorenz, Patrick Esser, and Björn Ommer. High-resolution image synthesis with latent diffusion models. In *Proceedings of the IEEE/CVF Conference on Computer Vision and Pattern Recognition*, pages 10684–10695, 2022. 1, 2, 6, 8, 13, 14
- [47] Chitwan Saharia, William Chan, Saurabh Saxena, Lala Li, Jay Whang, Emily Denton, Seyed Kamyar Seyed Ghasemipour, Burcu Karagol Ayan, S Sara Mahdavi, Rapha Gontijo Lopes, et al. Photorealistic text-to-image diffusion models with deep language understanding. *arXiv preprint arXiv:2205.11487*, 2022. 1, 2
- [48] Tim Salimans, Ian Goodfellow, Wojciech Zaremba, Vicki Cheung, Alec Radford, and Xi Chen. Improved techniques for training gans. *Advances in neural information processing systems*, 29, 2016. 4
- [49] Christoph Schuhmann, Richard Vencu, Romain Beaumont, Robert Kaczmarczyk, Clayton Mullis, Aarush Katta, Theo Coombes, Jenia Jitsev, and Aran Komatsuzaki. Laion-400m: Open dataset of clip-filtered 400 million image-text pairs. *arXiv preprint arXiv:2111.02114*, 2021. 2
- [50] Ramprasaath R Selvaraju, Michael Cogswell, Abhishek Das, Ramakrishna Vedantam, Devi Parikh, and Dhruv Batra. Grad-cam: Visual explanations from deep networks via gradient-based localization. In *Proceedings of the IEEE international conference on computer vision*, pages 618–626, 2017. 9
- [51] Hao Tan and Mohit Bansal. Lxmert: Learning cross-modality encoder representations from transformers. In *Proceedings of the 2019 Conference on Empirical Methods in Natural Language Processing and the 9th International Joint Conference on Natural Language Processing (EMNLP-IJCNLP)*, pages 5100–5111, 2019. 3
- [52] Volker Tresp, Sahand Sharifzadeh, Hang Li, Dario Konopatzki, and Yunpu Ma. The tensor brain: A unified theory of perception, memory, and semantic decoding. *Neural Computation*, 35(2):156–227, 2023. 2
- [53] Ramakrishna Vedantam, C Lawrence Zitnick, and Devi Parikh. Cider: Consensus-based image description evaluation. In *Proceedings of the IEEE conference on computer vision and pattern recognition*, pages 4566–4575, 2015. 2, 3, 4
- [54] Bram Wallace, Akash Gokul, Stefano Ermon, and Nikhil Naik. End-to-end diffusion latent optimization improves classifier guidance. *arXiv preprint arXiv:2303.13703*, 2023. 6
- [55] Peng Wang, An Yang, Rui Men, Junyang Lin, Shuai Bai, Zhikang Li, Jianxin Ma, Chang Zhou, Jingren Zhou, and Hongxia Yang. Unifying architectures, tasks, and modalities through a simple sequence-to-sequence learning framework. *arXiv preprint arXiv:2202.03052*, 2022. 1, 3
- [56] Zirui Wang, Jiahui Yu, Adams Wei Yu, Zihang Dai, Yulia Tsvetkov, and Yuan Cao. Simvln: Simple visual language model pretraining with weak supervision. *arXiv preprint arXiv:2108.10904*, 2021. 1, 3
- [57] Kelvin Xu, Jimmy Ba, Ryan Kiros, Kyunghyun Cho, Aaron Courville, Ruslan Salakhudinov, Rich Zemel, and Yoshua Bengio. Show, attend and tell: Neural image caption generation with visual attention. In *International conference on machine learning*, pages 2048–2057. PMLR, 2015. 1
- [58] Xingqian Xu, Zhangyang Wang, Eric Zhang, Kai Wang, and Humphrey Shi. Versatile diffusion: Text, images and variations all in one diffusion model. *arXiv preprint arXiv:2211.08332*, 2022. 3
- [59] Michihiro Yasunaga, Armen Aghajanyan, Weijia Shi, Rich James, Jure Leskovec, Percy Liang, Mike Lewis, Luke Zettlemoyer, and Wen-tau Yih. Retrieval-augmented multimodal language modeling. *arXiv preprint arXiv:2211.12561*, 2022. 1
- [60] Jiahui Yu, Zirui Wang, Vijay Vasudevan, Legg Yeung, Mojtaba Seyedhosseini, and Yonghui Wu. Coca: Contrastive captioners are image-text foundation models. *arXiv preprint arXiv:2205.01917*, 2022. 1, 3
- [61] Jiahui Yu, Yuanzhong Xu, Jing Yu Koh, Thang Luong, Gunjan Baid, Zirui Wang, Vijay Vasudevan, Alexander Ku, Yinfei Yang, Burcu Karagol Ayan, et al. Scaling autoregressive models for content-rich text-to-image generation. *arXiv preprint arXiv:2206.10789*, 2022. 2
- [62] Pengchuan Zhang, Xiujun Li, Xiaowei Hu, Jianwei Yang, Lei Zhang, Lijuan Wang, Yejin Choi, and Jianfeng Gao. Vinvl: Revisiting visual representations in vision-language models. In *Proceedings of the IEEE/CVF Conference on Computer Vision and Pattern Recognition*, pages 5579–5588, 2021. 1, 3
- [63] Susan Zhang, Stephen Roller, Naman Goyal, Mikel Artetxe, Moya Chen, Shuohui Chen, Christopher Dewan, Mona Diab, Xian Li, Xi Victoria Lin, et al. Opt: Open pre-trained trans-

- former language models. *arXiv preprint arXiv:2205.01068*, 2022. [9](#)
- [64] Yufan Zhou, Ruiyi Zhang, Changyou Chen, Chunyuan Li, Chris Tensmeyer, Tong Yu, Jiuxiang Gu, Jinhui Xu, and Tong Sun. Lafite: Towards language-free training for text-to-image generation. *arXiv preprint arXiv:2111.13792*, 2021. [2](#), [14](#)
- [65] Jun-Yan Zhu, Taesung Park, Phillip Isola, and Alexei A Efros. Unpaired image-to-image translation using cycle-consistent adversarial networks. In *Proceedings of the IEEE international conference on computer vision*, pages 2223–2232, 2017. [7](#)
- [66] Xizhou Zhu, Jinguo Zhu, Hao Li, Xiaoshi Wu, Hongsheng Li, Xiaohua Wang, and Jifeng Dai. Uni-perceiver: Pre-training unified architecture for generic perception for zero-shot and few-shot tasks. In *Proceedings of the IEEE/CVF Conference on Computer Vision and Pattern Recognition*, pages 16804–16815, 2022. [3](#)
- [67] Xueyan Zou, Zi-Yi Dou, Jianwei Yang, Zhe Gan, Linjie Li, Chunyuan Li, Xiyang Dai, Harkirat Behl, Jianfeng Wang, Lu Yuan, et al. Generalized decoding for pixel, image, and language. In *Proceedings of the IEEE/CVF Conference on Computer Vision and Pattern Recognition*, pages 15116–15127, 2023. [1](#)

Supplementary Material

A. Experimental Details

A.1. Implementation of Similarity Metrics

This subsection lists approaches for computing image-to-image similarities and text-to-text similarities. In the image-text-image and text-image-text tasks, the evaluation metrics and distance metrics are closely related, i.e., the evaluation metrics for one task serve as distance metrics for the other task. Hence, we present them jointly in this section.

CLIP: The CLIP ViT-L/14 model³ is pre-trained on a 400M text-image pair dataset. Specifically, we employ the outputs from the visual projection layer with an embedding size of 768 for the CLIP image encoder. For the CLIP text encoder, the outputs from the textual projection layer with an embedding size of 512 are used.

DINO: The pretrained DINO ViT-B/8 model⁴ are used to obtain the image embeddings. DINO has been trained on the images dataset in a self-supervised way and has shown superior performance on representation learning tasks. The input image size is set to 384 and the output embedding size to 768.

FID, IS: Following [46], the torch-fidelity library⁵ is used to compute the fidelity scores of the generated images.

SBERT: We use Sentence-BERT⁶ with embedding size of 384 and take the [CLS] embeddings from the last transformer layer as the representation for the input text.

WMD: We use the open implementation of NLTK library⁷ to compute WMD between a source sentence and a target sentence. Specifically, we use the *glove-wiki-gigaword* vector embeddings with 200 dimensions as the choice for the WMD. Since WMD is a distance metric rather than a score metric, we plot the y -axis in the reversed order to represent that the higher the y , the better the text, as shown in the second subfigure in Figure 3.

A.2. Details of Generation Models and Benchmarks

We use the NoCaps [1] validation set of 4500 images and a subset of 2000 images from the COCO Karpathy test split [27] to support the evaluation. For BLIP⁸, we use the ViT-L model finetuned for the image captioning task. For SD⁹, we use the weights sd-v1-4.ckpt and DDPM scheduler

³adapted from the public library <https://huggingface.co/docs/transformers/modeldoc/clip>

⁴adapted from <https://github.com/facebookresearch/dino>

⁵public implementation available from <https://github.com/toshas/torch-fidelity>

⁶public implementation from <https://huggingface.co/sentence-transformers/all-MiniLM-L6-v2>

⁷<https://www.nltk.org/>

⁸<https://github.com/salesforce/BLIP>

⁹<https://github.com/huggingface/diffusers>

with sampling steps of 50 and a guidance scale of 7.5. The output image size is 512. The number of minimal words is set to 5 and the maximum number of words is set to 30. We set $p=0.9$ in the Top- p strategy.

B. Impact of Parameter of Top- p Sampling

p	0.1	0.2	0.3	0.4	0.5
CIDEr	111.8	111.2	110.0	107.2	103.4
p	0.6	0.7	0.8	0.9	0.95
CIDEr	96.2	89.7	83.1	78.7	69.2

Table 6. Impact of p on the Top- p sampling performance of BLIP ViT-L.

Top- p sampling, which is also referred to as nucleus sampling, is a text generation method that samples words from a set of candidates whose cumulative probability exceeds a specified threshold p . By varying p , we achieve a trade-off between the diversity and accuracy of the generated text. Broadly speaking, larger values of p result in more diverse captions, whereas smaller values of p lead to less variable yet more accurate captions for an input image.

Note that in Table 2 of the BLIP paper [35], the Top- p sampling method is used to generate a diverse set of captions which are then utilized for bootstrapping the BLIP model. However, the evaluation result in that row is obtained by the beam search method. To examine the effect of p , we report the performance of BLIP ViT-L on the NoCaps dataset for image captioning, under different choices of p , in Table 6.

C. Influence of Sampling Methods for Image Captioning

Several sampling methods exist for generating text in the image captioning model. Apart from the Top- p sampling approach presented in the main text, we conduct a quantitative evaluation of two different sampling strategies, including Top- k [16] with $k=10$, and Tempered sampling [9, 39] with $T=0.7$. Each sampling method serves as a baseline. Table 7 verifies that our conclusion is solid across different sampling methods.

D. Impact of Number of Candidates N

We investigate the effect of the number of candidates N on our findings. We conduct experiments using the BLIP ViT-L model on the NoCaps dataset for image captioning, utilizing the Top- p sampling method. For image generation, we use the SD model and the DDPM scheduler. We sample N candidates for each input image or text in each experiment. We compare our approach to the baseline method, where a candidate is selected randomly.

Method	Nocaps								COCO			
	In-domain		Near-domain		Out-domain		Overall		Karpathy Test			
	CIDEr	SPICE	CIDEr	SPICE	CIDEr	SPICE	CIDEr	SPICE	B@3	B@4	CIDEr	SPICE
Top- <i>k</i> Sampling	79.5	13.2	78.4	12.4	83.4	11.7	79.6	12.4	39.7	28.1	108.4	20.9
Ours	84.3	13.5	81.6	12.8	91.6	12.7	84.0	12.9	40.1	28.7	111.6	21.5
Gain (%)	+6.0	+2.3	+4.1	+3.2	+9.8	+8.5	+5.5	+4.0	+1.1	+2.3	+2.9	+2.9
Tempered Sampling	83.9	13.2	82.7	12.7	89.8	12.0	84.3	12.6	33.0	22.2	92.4	19.5
Ours	87.8	13.4	87.0	13.1	98.1	12.8	89.3	13.1	33.6	22.8	95.4	20.4
Gain (%)	+4.6	+1.5	+5.2	+3.1	+9.2	+6.7	+5.9	+4.0	+1.8	+2.6	+3.2	+4.7

Table 7. Comparison of different sampling methods and our proposed method on Nocaps and COCO datasets. Our method outperforms every sampling method on all metrics. The relative gain of our method compared to each sampling method is given in the last row in each block. B@*k*: BLEU@*k*.

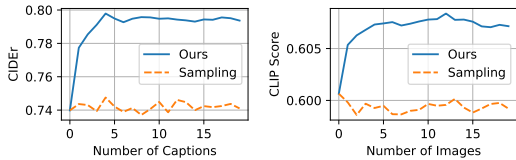


Figure 9. Evaluation of the choice of the number of sample candidates.

Figure 9 depicts the impact of the number of candidates on image-text-image (left) and text-image-text (right) tasks. The figure (left) shows the image captioning score (*y*-axis) for our approach and the baseline method, with the *x*-axis representing the number of candidate captions for each input image. As shown in the figure, the performance of the baseline method remains consistent as it randomly samples captions with varying qualities. Conversely, our approach improves significantly after the number of captions has reached around five. When the number of candidates is limited, there may not be enough high-quality captions to choose from, resulting in lower performance. Nevertheless, our approach remains effective even in that stage. After acquiring a reasonable number of candidates, our method consistently outperforms the baseline method by a significant margin. A similar conclusion can be inferred for the text-image-text task, as demonstrated on the right side of the figure.

E. Qualitative Results for Image and Text Generation

To reinforce the findings in Section 3, we provide additional qualitative examples on the NoCaps dataset. The annotations and explanations for each figure are included in their respective captions. Figure 10 shows both positive examples and negative examples for the image-text-image task, whereas Figure 11 presents visualizations for the text-image-text task. All results are obtained from BLIP ViT-L and SD models.

F. Analysis of Different Image-to-Text and Text-to-Image Generative Models

We conduct further experiments with different image captioning and text-to-image models. Table 8 shows the result of BLIP with a VAE-based image generative model LAFITE for the image-text-image task, as well as SD with BLIP-2 for the text-image-text task. In general, our finding, that better reconstruction leads to better generation performance, still holds. We find that SD performs better than LAFITE, very likely due to its larger training data. When coupled with BLIP-2, SD improved the performance upon the baseline, but it performed worse than that in the case of BLIP.

Text Generation					
I2T	T2I	I-C	N-C	O-C	E-C
Baseline		75.1	72.4	78.7	74.1
BLIP [35]	SD [46]	77.3	78.3	88.8	80.3
BLIP [35]	LAFITE [64]	75.4	76.2	82.9	77.4
Image Generation					
T2I	I2T	CLIP↓	FID↓	IS↑	
Baseline		40.54	32.37	41.19 ± 2.91	
SD [46]	BLIP [35]	33.47	29.59	45.64 ± 2.40	
SD [46]	BLIP-2 [34]	39.41	31.34	42.34 ± 2.23	

Table 8. Comparison of different combinations of generation models. We evaluate two image captioning models and two image generation models on the NoCaps dataset. I2T: Image-to-text model. T2I: Text-to-image model. I-C/N-C/O-C/E-C: In-/Near-/Out-/Entire-domain CIDEr.

G. Implementations of Tokenizer Transformation

We elaborate on the gradient backpropagation process between the output of BLIP and the input of SD, shown on the left side of Figure 6. Our framework includes three types of text tokenizers: BLIP utilizes the word-piece tokenizing method; BLIP-2 uses the byte-pair-encoding tokenizing method; SD employs the CLIP tokenizer, which uses the word-level tokenizing strategy. One of the challenges we faced is to align the output token distributions from BLIP with those from SD, allowing SD to interpret

the output of BLIP. To address this issue, we use these tokenization strategies to tokenize each sentence in the COCO training set and learn a one-to-one hard-coded mapping from a source token to a target token. Despite using different strategies, we found that these tokenizing methods have a high ratio of overlapping between tokens. Specifically, when applied to the COCO training set, more than 60% captions can be tokenized into the same set of tokens for BLIP and SD. For unmatched tokens, we map them to the most similar ones or to the [UNK] token. We visually examined this method by generating images conditioned on token distributions and found it to be practical. Additionally, we remove the prefix tokens of BLIP, *a photo of*, and add [BOS] and [EOS] tokens for SD.

H. Discussion on the Loss Function

Parameter Update While optimizing \mathcal{L}_{IR} for image captioning, both SD and BLIP are trained. \mathcal{L}_{TG} only updates the parameters of BLIP. Likewise, both SD and BLIP are trained when optimizing \mathcal{L}_{TR} , and only SD is updated by \mathcal{L}_{IG} . The reasons for training SD in \mathcal{L}_{IR} are twofold. First, SD needs to adapt to new distributions coming from BLIP. As in the standard training, the input of BLIP is discrete tokens. Whereas in our approach, the input is token distributions. Second, SD could be improved because of additional training data sampled from BLIP. In addition, since they are refreshed at each iteration, one model is able to provide better samples to train the other model throughout the training.

Connection to CycleGAN CycleGAN is a generative model that learns bidirectional mappings from domain X to domain Y , where X and Y are images. Its cyclic loss ensures that the mapping between the input and output domains is consistent, i.e., if we take an image from domain X , pass it through the generator network to obtain an image in domain Y , and then pass that image through the generator network again to obtain an image in domain X , we should obtain an image that is similar to the original image in domain X . Likewise, we aim to enforce consistent mapping between the input and output domains, but we deal with two distinct domains, i.e., image and language, which may require much more complex mapping. In addition, we also optimize a single objective, similar to CycleGAN which is trained on the weighted cyclic loss and adversarial loss. CycleGAN employs a hyperparameter λ to control the relative importance of the cyclic loss to the adversarial loss, we found that a similar weighting did not yield substantial differences in performance in our work. Therefore we do not adjust this hyperparameter in our approach.

Pseudo-Code The pseudo-code of our train framework is presented in Algorithm 1.

Algorithm 1 Training Framework

Model UNet ϵ_ψ , SD’s Text Encoder π , BLIP b_θ
Input an image-text pair $(\mathbf{x}_0, \mathbf{y})$

- 1: **repeat**
- # Image-Text-Image (BLIP \rightarrow SD)
- 2: $\mathbf{x}_0, \mathbf{y} \sim q(\mathbf{x}_0, \mathbf{y})$ \triangleright Sample an image-text pair from the dataset
- 3: $\hat{\mathbf{y}} = b_\theta(\mathbf{x}_0, \tilde{\mathbf{y}})$ $\triangleright \hat{\mathbf{y}} \in \mathbb{R}^{L \times V}$: Output token distribution.
 $\tilde{\mathbf{y}}$: (causal) masked text input
- 4: $\mathcal{L}_1 = \text{CE}(\mathbf{y}, \hat{\mathbf{y}})$ \triangleright CE: cross entropy loss
- 5: $\mathbf{c} = \pi(\hat{\mathbf{y}})$ \triangleright Text encoder encodes BLIP’s output into embeddings
- 6: $t \sim \text{Uniform}(\{1, \dots, T\})$ \triangleright Sample a timestep for the diffusion process
- 7: $\epsilon \sim \mathcal{N}(\mathbf{0}, \mathbf{I})$ \triangleright Sample noise for timestep t
- 8: $\mathbf{x}_t = \sqrt{\alpha_t} \mathbf{x}_0 + \sqrt{1 - \alpha_t} \epsilon$ \triangleright Add noise to image
- 9: $\hat{\epsilon} = \epsilon_\psi(\mathbf{x}_t, \mathbf{c})$ \triangleright UNet predicts noise $\hat{\epsilon}$ from the noisy image \mathbf{x}_t
- 10: $\mathcal{L}_2 = \|\epsilon - \hat{\epsilon}\|^2$
- # Text-Image-Text (SD \rightarrow BLIP)
- 11: $\mathbf{x}_0, \mathbf{y} \sim q(\mathbf{x}_0, \mathbf{y})$ \triangleright Sample an image-text pair from the dataset
- 12: $\mathbf{c} = \pi(\mathbf{y})$ \triangleright Text encoder encodes input text into embeddings
- 13: $t \sim \text{Uniform}(\{1, \dots, T\})$ \triangleright Sample a timestep for the diffusion process
- 14: $\epsilon \sim \mathcal{N}(\mathbf{0}, \mathbf{I})$ \triangleright Sample noise for timestep t
- 15: $\mathbf{x}_t = \sqrt{\alpha_t} \mathbf{x}_0 + \sqrt{1 - \alpha_t} \epsilon$ \triangleright Add noise to image
- 16: $\hat{\epsilon} = \epsilon_\psi(\mathbf{x}_t, \mathbf{c})$ \triangleright UNet predicts noise $\hat{\epsilon}$ from the noisy image \mathbf{x}_t
- 17: $\mathcal{L}_3 = \|\epsilon - \hat{\epsilon}\|^2$
- 18: $\hat{\mathbf{x}}_0 = \frac{1}{\sqrt{\alpha_t}}(\mathbf{x}_t - \sqrt{1 - \alpha_t} \hat{\epsilon})$ \triangleright 1-step approximation of \mathbf{x}_0
- 19: $\mathcal{L}_4 = \text{CE}(\mathbf{y}, b_\theta(\hat{\mathbf{x}}_0, \tilde{\mathbf{y}}))$ $\triangleright \tilde{\mathbf{y}}$: (causal) masked text input
- 20: Take gradient descent step on
 BLIP: $\nabla_\theta(\mathcal{L}_1 + \mathcal{L}_2 + \mathcal{L}_3 + \mathcal{L}_4) = \nabla_\theta(\mathcal{L}_1 + \mathcal{L}_2 + \mathcal{L}_4)$
 SD: $\nabla_\psi(\mathcal{L}_1 + \mathcal{L}_2 + \mathcal{L}_3 + \mathcal{L}_4) = \nabla_\psi(\mathcal{L}_2 + \mathcal{L}_3 + \mathcal{L}_4)$
- 21: **until** converged
- 22: **return** ψ, θ

I. Ablation Study

Table 9 summarizes the different losses and weight-freezing strategies, highlighting that improvement comes from the proposed reconstruction loss. For simplicity, we only list the effect of different settings on BLIP. Our default setting jointly optimizes both pipelines with both models trainable $p_1 : \mathbf{I} \xrightarrow{\text{BLIP}} \mathbf{T}(L_{TG}) \xrightarrow{\text{SD}} \mathbf{I}(L_{IR})$, and $p_2 : \mathbf{T} \xrightarrow{\text{SD}} \mathbf{I}(L_{IG}) \xrightarrow{\text{BLIP}} \mathbf{T}(L_{TR})$. The third column in the table shows the training signals that BLIP can receive from the two pipelines under the specific setting. ”-” means that loss has no effect as the model is frozen.

Weights Update				Loss Function				Effect on BLIP	Experiment	CIDEr
BLIP ^{p1}	SD ^{p1}	SD ^{p2}	BLIP ^{p2}	L_{TG}	L_{IR}	L_{IG}	L_{TR}			
✓	✓	✓	✓	✓	✓	✓	✓	p_1 : ground truth + reconstruction p_2 : augmentation	Ours, Tab. 4	111.8
✓	×	×	×	✓	×	-	-	p_1 : ground truth	Tab. 4	109.7
✓	×	✓	×	✓	✓	✓	✓	p_1 : ground truth + reconstruction	Ablation	110.9
×	✓	×	✓	-	✓	-	✓	p_2 : augmentation	Ablation	110.2
✓	×	×	×	×	✓	-	-	p_1 : reconstruction	Tab. 6	102.3

Table 9. Analysis of different training paradigms of loss terms and model frozen strategies.

J. Qualitative Results for Training Framework

We provide additional qualitative examples of image captioning and image generation by our trained framework in Figure 12 and Figure 13, respectively. Detailed annotations and explanations can be found in the corresponding figure captions.

Input	Sample #1	Sample #2	Sample #3	Sample #4	Sample #5
	<p>the pink golf cart is parked outside a trailer</p> <p>CIDEr: 348.8 CLIP Text: 0.849</p>	<p>the small golf cart has pink paint and has a name written on it</p> <p>CIDEr: 152.4 CLIP Text: 0.821</p>	<p>a pink golf cart with a girly sign on the side</p> <p>CIDEr: 343.4 CLIP Text: 0.864</p>	<p>a pink cart that is sitting outside</p> <p>CIDEr: 141.7 CLIP Text: 0.771</p>	
	<p>a black and yellow bird sitting in a tree</p> <p>CIDEr: 307.1 CLIP Text: 0.805</p>	<p>a yellow and black bird perched in a tree</p> <p>CIDEr: 211.1 CLIP Text: 0.869</p>	<p>two birds perched on a tree branch in the forest</p> <p>CIDEr: 85.8 CLIP Text: 0.639</p>	<p>the two birds are sitting on the branch</p> <p>CIDEr: 62.4 CLIP Text: 0.581</p>	
	<p>colorful oriental lanterns hung from the ceiling and light the room</p> <p>CIDEr: 139.5 CLIP Text: 0.735</p>	<p>many different colorful hanging lanterns on the ceiling</p> <p>CIDEr: 178.5 CLIP Text: 0.784</p>	<p>brightly lit lanterns on the ceiling of a shop</p> <p>CIDEr: 156.8 CLIP Text: 0.725</p>	<p>several colorful lamps with picture frames hanging</p> <p>CIDEr: 31.7 CLIP Text: 0.590</p>	
	<p>three bottles of milk on a shelf in a store</p> <p>CIDEr: 260.4 CLIP Text: 0.764</p>	<p>a few bottles of cow milk sitting in a row</p> <p>CIDEr: 116.6 CLIP Text: 0.647</p>	<p>milk products are on a shelf in a supermarket</p> <p>CIDEr: 86.3 CLIP Text: 0.652</p>	<p>a display in a grocery store with several different drinks</p> <p>CIDEr: 5.4 CLIP Text: 0.534</p>	
	<p>a close up of french toast with strawberries</p> <p>CIDEr: 333.6 CLIP Text: 0.825</p>	<p>plate of french toast topped with powdered sugar and sliced strawberries</p> <p>CIDEr: 297.1 CLIP Text: 0.858</p>	<p>french toast with strawberries and powdered sugar on a white plate</p> <p>CIDEr: 366.6 CLIP Text: 0.862</p>	<p>a white plate with a white dish of food and some strawberries</p> <p>CIDEr: 69.6 CLIP Text: 0.629</p>	
	<p>a close up of a gnome on a porch</p> <p>CIDEr: 150.3 CLIP Text: 0.590</p>	<p>a gnome statue standing next to a flower pot</p> <p>CIDEr: 190.5 CLIP Text: 0.796</p>	<p>the garden gnome is standing on the pavement with his arms out</p> <p>CIDEr: 156.6 CLIP Text: 0.568</p>	<p>a statue and potted plant next to steps</p> <p>CIDEr: 42.8 CLIP Text: 0.596</p>	
	<p>a close up of an otter's face in water</p> <p>CIDEr: 152.1 CLIP Text: 0.717</p>	<p>an otter that is sitting in the water</p> <p>CIDEr: 207.7 CLIP Text: 0.822</p>	<p>a river otter in the water looking to his left</p> <p>CIDEr: 144.2 CLIP Text: 0.819</p>	<p>a close up shot of an animal in the water</p> <p>CIDEr: 31.2 CLIP Text: 0.508</p>	
	<p>a glass of beer sitting on a table</p> <p>CIDEr: 290.2 CLIP Text: 0.763</p>	<p>a beverage sitting in a glass on top of a table</p> <p>CIDEr: 46.0 CLIP Text: 0.708</p>	<p>a close up of a glass of alcohol on a table</p> <p>CIDEr: 42.1 CLIP Text: 0.623</p>	<p>a small orange slice in a glass sitting on top of a wooden table</p> <p>CIDEr: 56.5 CLIP Text: 0.571</p>	
	<p>people are sitting on a snowmobile and waiting for something</p> <p>CIDEr: 160.0 CLIP Text: 0.702</p>	<p>people standing on a snow bike in front of a hotel</p> <p>CIDEr: 124.6 CLIP Text: 0.618</p>	<p>a man and two women are riding on a snow bike</p> <p>CIDEr: 38.1 CLIP Text: 0.707</p>	<p>two men and a woman sit on the front of a ski machine outside of a building</p> <p>CIDEr: 11.1 CLIP Text: 0.630</p>	
	<p>a knife and two fresh carrots next to each other</p> <p>CIDEr: 116.1 CLIP Text: 0.734</p>	<p>four different types of carrots on a cutting board</p> <p>CIDEr: 69.8 CLIP Text: 0.633</p>	<p>three different colored vegetables laying next to a knife</p> <p>CIDEr: 93.2 CLIP Text: 0.675</p>	<p>the vegetables have been cut into two large ones</p> <p>CIDEr: 11.9 CLIP Text: 0.605</p>	
	<p>a baby lemur up in a tree</p> <p>CIDEr: 35.3 CLIP Text: 0.629</p>	<p>a black and white lemur on top of a tree</p> <p>CIDEr: 29.9 CLIP Text: 0.594</p>	<p>a monkey up in a tree looking at the camera</p> <p>CIDEr: 176.4 CLIP Text: 0.763</p>	<p>a large gray and white monkey standing on top of a tree</p> <p>CIDEr: 156.0 CLIP Text: 0.624</p>	
	<p>a person carrying an umbrella walking along a wooden bridge</p> <p>CIDEr: 152.7 CLIP Text: 0.733</p>	<p>woman holding umbrella walking on wooden bridge in the sun</p> <p>CIDEr: 158.3 CLIP Text: 0.749</p>	<p>a man is walking across the bridge with an umbrella</p> <p>CIDEr: 195.5 CLIP Text: 0.723</p>	<p>a woman with an umbrella walking across a bridge</p> <p>CIDEr: 217.9 CLIP Text: 0.800</p>	

Figure 10. Examples for the image-text-image task using Top- p sampling. The first column displays the input images, followed by the generated caption and its corresponding generated image. We rank the generated text-image pairs based on the similarity of the images and show the score of the caption below each text. In the first row, *golf car* in the first sample is a more accurate description than *cart* in the fifth sample so that the first generated image is closer to the input image. Additionally, we show a few failed examples in the last two rows.

Input	Sample #1	Sample #2	Sample #3	Sample #4	Sample #5
People are standing around a black luxury vehicle.	 Visual Score: 0.559 FID: 179.6	 Visual Score: 0.489 FID: 209.5	 Visual Score: 0.549 FID: 213.4	 Visual Score: 0.456 FID: 217.2	 Visual Score: 0.452 FID: 152.1
A woman dressed in a black outfit is playing the harp on a stage	 Visual Score: 0.680 FID: 55.2	 Visual Score: 0.642 FID: 97.8	 Visual Score: 0.609 FID: 71.2	 Visual Score: 0.356 FID: 575.0	 Visual Score: 0.482 FID: 453.2
A three layer white cake with blue, pink, red and green figures on top.	 Visual Score: 0.610 FID: 269.6	 Visual Score: 0.668 FID: 280.7	 Visual Score: 0.644 FID: 333.1	 Visual Score: 0.544 FID: 333.9	 Visual Score: 0.533 FID: 382.9
A crowd stands near a memorialized motorcycle that has a passenger car attached to it.	 Visual Score: 0.722 FID: 126.0	 Visual Score: 0.583 FID: 153.9	 Visual Score: 0.676 FID: 111.2	 Visual Score: 0.611 FID: 146.8	 Visual Score: 0.428 FID: 216.0
A saxophone lays on a glass table in front of a window, and we can see its reflection in the table.	 Visual Score: 0.614 FID: 106.9	 Visual Score: 0.592 FID: 160.4	 Visual Score: 0.772 FID: 71.5	 Visual Score: 0.410 FID: 389.2	 Visual Score: 0.437 FID: 303.5
A black classic car with a black license plate.	 Visual Score: 0.799 FID: 99.1	 Visual Score: 0.610 FID: 207.0	 Visual Score: 0.719 FID: 213.4	 Visual Score: 0.596 FID: 138.9	 Visual Score: 0.541 FID: 136.7
A curled up pretzel on a desk next to a computer mouse and wires.	 Visual Score: 0.668 FID: 140.9	 Visual Score: 0.754 FID: 93.2	 Visual Score: 0.592 FID: 174.8	 Visual Score: 0.652 FID: 100.7	 Visual Score: 0.452 FID: 348.8
A red bag of buttered popcorn sitting in a chair.	 Visual Score: 0.825 FID: 314.5	 Visual Score: 0.832 FID: 290.5	 Visual Score: 0.819 FID: 250.3	 Visual Score: 0.751 FID: 261.3	 Visual Score: 0.487 FID: 365.3
A hockey player skating with a hockey puck.	 Visual Score: 0.643 FID: 45.8	 Visual Score: 0.739 FID: 155.5	 Visual Score: 0.520 FID: 144.9	 Visual Score: 0.624 FID: 67.0	 Visual Score: 0.574 FID: 88.7
Three young men are in a room playing the bass, the guitar and a trombone.	 Visual Score: 0.473 FID: 130.8	 Visual Score: 0.568 FID: 130.8	 Visual Score: 0.559 FID: 236.8	 Visual Score: 0.399 FID: 186.3	 Visual Score: 0.488 FID: 153.2
A person is sitting in a chair in front of audio equipment.	 Visual Score: 0.531 FID: 302.9	 Visual Score: 0.512 FID: 194.6	 Visual Score: 0.496 FID: 235.4	 Visual Score: 0.602 FID: 354.8	 Visual Score: 0.721 FID: 305.4
A black bottle of perfume with some floral details	 Visual Score: 0.512 FID: 311.1	 Visual Score: 0.463 FID: 415.3	 Visual Score: 0.552 FID: 299.0	 Visual Score: 0.533 FID: 301.0	 Visual Score: 0.643 FID: 206.5

Figure 11. Examples for the text-image-text task. The first column shows the input text, followed by generated image and its corresponding generated text. We rank the generated image-text pairs by the similarity of the text and show the score of the image in the box. As shown in the first line, the image in the first sample represents the input text better than the image in the fifth sample, and the similarity of the reconstructed text reflected this comparison. Further, we show some failed examples in the last two rows.

	<p>GT: A little girl with long straight reddish brown hair tilts her head to the right and smiles at us.</p> <p>BLIP: a close up of a child with a toothbrush</p> <p>Ours: a little girl with a smile on her face</p>		<p>GT: Three men in sports uniforms smiling next to each other</p> <p>BLIP: a group of men standing next to each other on a podium</p> <p>Ours: three men standing on a podium with medals around their necks</p>		<p>GT: A man with a ponytail that is playing the saxophone.</p> <p>BLIP: a man playing a trumpet in a black and white photo</p> <p>Ours: a man playing a saxophone in a black and white photo</p>
	<p>GT: People on motorcycles in the street with helmets.</p> <p>BLIP: a group of people riding scooters down a street</p> <p>Ours: a group of people riding motorcycles down a street</p>		<p>GT: A little girl in a blue shirt preparing to shoot a basket.</p> <p>BLIP: a group of young people playing a game of basketball</p> <p>Ours: a young girl holding a basketball in a gym</p>		<p>GT: A woman standing beside an vintage two door car.</p> <p>BLIP: a woman standing in front of an old car</p> <p>Ours: a woman in a dress and hat standing next to an old car</p>
	<p>GT: A man wearing a jacket and doing tricks on a bike.</p> <p>BLIP: a man riding a bike down the middle of a street</p> <p>Ours: a man is doing a trick on a bicycle</p>		<p>GT: An empty cup of coffee on a saucer by a phone.</p> <p>BLIP: a cup of coffee sitting on top of a white saucer</p> <p>Ours: a cup of coffee on a saucer next to a cell phone</p>		<p>GT: Two zebras standing close together on dirt surface.</p> <p>BLIP: a couple of zebra standing next to each other</p> <p>Ours: two zebras standing next to each other on a dirt road</p>
	<p>GT: Pilot and smiling copilot sitting in cockpit of airplane.</p> <p>BLIP: a couple of people that are sitting in a plane</p> <p>Ours: a man and a woman sitting in the cockpit of an airplane</p>		<p>GT: Woman with red hair holding silver digital camera in front of her face.</p> <p>BLIP: a woman taking a picture of herself with a camera</p> <p>Ours: a woman holding a camera in front of her face</p>		<p>GT: A person on a motorized vehicle in a red sweater.</p> <p>BLIP: a man riding an electric scooter in a parking lot</p> <p>Ours: a man on a segway at a car show</p>
	<p>GT: A small plant grows out of some dirt in a small pot.</p> <p>BLIP: a small green tree sitting on top of a wooden table</p> <p>Ours: a bonsai tree in a pot on a table</p>		<p>GT: Three women are dancing while wearing a black and white dress.</p> <p>BLIP: a group of people that are standing on a stage</p> <p>Ours: a group of women in black and white dresses dancing</p>		<p>GT: A man drinking a beer on a golf cart.</p> <p>BLIP: a man sitting in a golf cart on a golf course</p> <p>Ours: a man sitting in a golf cart drinking a beverage</p>
	<p>GT: Glass curtained windows, rest above new-looking brick siding, fronted by a pair of healthy sunflowers.</p> <p>BLIP: a large yellow sunflower in front of a brick wall</p> <p>Ours: two sunflowers in front of a brick wall</p>		<p>GT: A man skis downhill on icy snow, one winter.</p> <p>BLIP: a man riding skis down a snow covered slope</p> <p>Ours: a person in an orange and white ski suit skiing down a hill</p>		<p>GT: A woman in black rides a brightly painted cruiser motorcycle with a small dog on her lap.</p> <p>BLIP: a man riding a motorcycle down a street</p> <p>Ours: a person riding a motorcycle with a dog on the back</p>
	<p>GT: A closeup of a large lobster in water</p> <p>BLIP: a close up of a red and white crab under water</p> <p>Ours: a close up of a red and white lobster</p>		<p>GT: Grey dolphin swimming with half body out of water</p> <p>BLIP: a dolphin swimming in the ocean near a boat</p> <p>Ours: a dolphin is swimming in the blue water</p>		<p>GT: Empty living room with black sofa and yellow striped curtains</p> <p>BLIP: a living room filled with furniture and a flat screen tv</p> <p>Ours: a living room with a black couch and a television</p>
	<p>GT: A chef stands by an appliance making something good.</p> <p>BLIP: a man standing in front of a pizza oven</p> <p>Ours: a man in a red apron standing in front of a machine</p>		<p>GT: A white bicycle chained to a lamp post.</p> <p>BLIP: a bicycle parked next to a pole on a city street</p> <p>Ours: a white bicycle is chained to a pole</p>		<p>GT: A blonde woman wearing a blue and white striped shirt and pink scarf.</p> <p>BLIP: a woman with a cell phone in her hand</p> <p>Ours: a woman wearing a blue and white striped shirt</p>
	<p>GT: A white limousine driving down a road.</p> <p>BLIP: a white limousine parked on the side of a road</p> <p>Ours: a white car parked on the side of a road</p>		<p>GT: A person sitting on one of the four stools standing in a line</p> <p>BLIP: a woman sitting on a stool next to two stools</p> <p>Ours: a woman sitting at a bar with her legs crossed</p>		<p>GT: Large piece of brown cake on top of a tray.</p> <p>BLIP: a loaf of bread sitting on top of a metal rack</p> <p>Ours: a close up of a piece of food on a rack</p>
	<p>GT: A red grandfather clock is sitting by a white wall.</p> <p>BLIP: a red grandfather clock sitting on top of a wooden floor</p> <p>Ours: a tall red clock sitting on top of a wooden floor</p>		<p>GT: Cookies are on a tray being cooked under heat.</p> <p>BLIP: a close up of chocolate chip cookies on a baking sheet</p> <p>Ours: a bunch of cookies that are on a table</p>		<p>GT: A bunch of colorful balloons stand outside of tall buildings.</p> <p>BLIP: a bunch of green and yellow balloons in front of a building</p> <p>Ours: a bunch of balloons that are in the air</p>

Figure 12. Qualitative results for image captioning. We compare the performance of our approach and BLIP ViT-B baseline. A ground truth (GT) caption is given for each image. On average, our method provides more accurate descriptions for input images. The last two rows show examples of our model performing worse than the baseline method.

Input	Ours				SD			
A green car parked outside of a house.								
A kitchen with a table with chairs and a ceiling fan.								
White translucent jellyfish light up the darkness deep below the water.								
Man is enjoying playing while wearing their helmet.								
A dresser has some books on the top of it.								
A clock stands next to a white wall on wood floor.								
The lifeguard is sitting in a high chair with chairs and umbrellas behind him.								
Having a picnic outside your car is fun.								
Kitchen utensils alongside food in a large table								
A grey and white two story house between a grey fence with green bushes around the fence								

Figure 13. Qualitative results for image generation. We compare the original SD model with our finetuned model. Each row displays firstly the input text, followed by four images generated by our approach, and four images generated by the SD baseline. We can see that compared with the baseline method, the image generated by our method better reflects the semantics of the input text.